

Minimum thickness of flat plates considering construction load effect

Hyeon-Jong Hwang^{1,2a}, Gao Ma^{1b} and Chang-Soo Kim^{*3}

¹College of Civil Engineering and Hunan Provincial Key Lab on Damage Diagnosis for Engineering Structures, Hunan Univ., Yuelu Mountain, Changsha, Hunan 410082, P.R. China

²Engineering Research Institute, Seoul National Univ., Seoul 151-744, Republic of Korea

³School of Architecture, Seoul National University of Science and Technology, 232 Gongreung-ro, Nowon-gu, Seoul 01811, Republic of Korea

(Received March 22, 2018, Revised November 23, 2018, Accepted November 29, 2018)

Abstract. In the construction of flat plate slabs, which are widely used for tall buildings but have relatively low flexural stiffness, serviceability problems such as excessive deflections and cracks are of great concern. To prevent excessive deflections at service load levels, current design codes require the minimum slab thickness, but the requirement could be unconservative because it is independent on loading and elastic modulus of concrete, both of which have significant effects on slab deflections. In the present study, to investigate the effects of the construction load of shored slabs, reduced flexural stiffness and moment distribution of early-age slabs, and creep and shrinkage of concrete on immediate and time-dependent deflections, numerical analysis was performed using the previously developed numerical models. A parametric study was performed for various design and construction conditions of practical ranges, and a new minimum permissible thickness of flat plate slabs was proposed satisfying the serviceability requirement for deflection. The proposed minimum slab thickness was compared with current design code provisions and numerical analysis results, and it agreed well with the numerical analysis results.

Keywords: flat plate slab; construction load; immediate deflection; time-dependent deflection; minimum thickness

1. Introduction

The flat plate system has been widely used in the construction of tall buildings to lower story-heights, improve constructability, and shorten construction periods. Because the flexural stiffness of flat plate slabs is relatively low, serviceability problems such as excessive deflections and cracks may occur. To prevent excessive deflections at service load levels, current design codes such as ACI 318 (2014) and Eurocode 2 (2004) specify limitations on the minimum slab thickness and maximum total deflection including immediate and time-dependent (creep and shrinkage) deflections. However, since the requirement of ACI 318 (2014) for the minimum slab thickness is independent on loading and elastic modulus of concrete, both of which have significant effects on deflections, the ACI requirement could be unconservative for long-span flat plate slabs under high service load levels (Lee and Scanlon 2010). Particularly, since early-age concrete has low strength and stiffness, the construction load effect on early-age slabs is critical for cracking and deflections (Gardner and Fu 1987, Kang *et al.* 2003, Kim 2009, Hwang *et al.* 2016, Kim and Kang 2017). Thus, in the calculation of the minimum slab thickness and total deflection of flat plate slabs, 1) the construction load effect on the immediate deflection and damages at early ages and 2) the creep and

shrinkage effect on the time-dependent deflection at early ages (a large amount of creep and shrinkage develops rapidly during the first few months after concrete casting and initial loading) need to be considered.

Various studies have been performed to predict the construction load imposed on shored slabs. The construction load is primarily affected by the number of shored slabs, construction cycle (period per story), and material properties of early-age concrete (ACI 347 2005). Grundy and Kabaila (1963) and Mosallam and Chen (1991) considered the slab stiffness ratio to distribute a newly superimposed construction load to shored slabs. Liu and Chen (1985) and El-Shahhat and Chen (1992) performed finite element analysis for slabs connected by shores, and investigated the effect of the shore stiffness on the construction load imposed on each slab. Park *et al.* (2011) estimated the construction load considering the number of shored slabs, construction cycle, shore stiffness, slab cracking, and material properties of early-age concrete.

The immediate and time-dependent deflections are strongly affected by the effective stiffness of early-age slabs. Particularly, in early-age slabs showing low strength and stiffness at low temperatures, the construction load could cause flexural damages and excessive deflections (Carino and Lew 1983, Mehta and Monteiro 2006), which reduce the effective stiffness of slabs. Hossain and Vollum (2002) and Hossain *et al.* (2011) proposed analysis methods for slab deflections based on CEB-FIP MC90 (1993) and ACI 318 (2014) models, and compared the predictions with the measured deflections of a 6-story flat plate structure. Gilbert (1999) and Lee *et al.* (2007) reported that the ACI 318 provision does not accurately evaluate the effective stiffness, tension stiffening, creep, and shrinkage, and

*Corresponding author, Ph.D., Associate professor
E-mail: changsookim@seoultech.ac.kr

^aPh.D., Associate professor

^bPh.D., Associate professor

underestimates deflections of early-age slabs. Park *et al.* (2012) reported that deflections of early-age slabs can be accurately predicted by using the material properties of early-age concrete measured from the material test and the creep and shrinkage models of ACI 209R-92 (1992).

In a previous research, Hwang *et al.* (2016) developed a numerical analysis method to predict deflections of flat plate slabs considering the variation of the construction load, reduced stiffness of slabs under construction, moment redistribution due to slab cracking, and creep and shrinkage of concrete. For verification, the predictions were compared with the measured deflections of two actual flat plate buildings under construction.

In the present study, to propose the minimum thickness of flat plate slabs satisfying the ACI requirement for serviceability (i.e., maximum total deflection), a parametric study was performed by numerical analysis. To this end, the previously developed numerical analysis method of Hwang *et al.* (2016) was used, and the total deflection of flat plate slabs under various design and construction conditions was examined. The proposed minimum slab thickness was compared with current design code provisions.

2. Numerical analysis

2.1 Existing design methods

Table 1 presents the minimum slab thickness specified in existing design methods of ACI 318 (2014), Eurocode 2 (2004), and Scanlon and Lee (2006). ACI 318 (2014) defines the minimum slab thickness h depending on the clear span L_n , yield strength f_y of reinforcement, and slab location, but the effects of loading and concrete strength are not considered. For slabs not satisfying the minimum slab thickness, the total deflection including immediate and time-dependent deflections occurring after attachment of nonstructural elements is limited not to exceed $L/480$ (L = span). Eurocode 2 (2004) limits the span-to-thickness ratio L/h as a function of concrete strength f_c' and reinforcement ratio ρ . For the span of exceeding 8.5 m, which is expected to support more partitions and be damaged by excessive deflections, the calculated L/h should be multiplied by $8.5/L_{eff}$ (L_{eff} = effective span in meters). To prevent damages of adjacent parts, the total deflection is limited not to exceed $L/500$. On the other hand, in the Scanlon and Lee's model (2006), the effect of sustained and live loads is directly considered.

For the calculation of the time-dependent deflection resulting from creep and shrinkage, ACI 318 (2014) provides a simple factor which is multiplied to the immediate deflection. On the other hand, Eurocode 2 (2004) uses the reduced elastic modulus of concrete due to creep, increased curvature due to shrinkage, and coefficient for sustained load in the calculation of the time-dependent deflection.

2.2 Numerical analysis procedure

For exact prediction of slab deflections, the immediate deflection affected by the degree of cracking at early ages

Table 1 Minimum slab thickness of existing design methods

	f_y	Exterior panels		Interior panels
		Without edge beams	With edge beams	
ACI 318 (2014)	280 MPa	$L_n / 33$	$L_n / 36$	$L_n / 36$
	420 MPa	$L_n / 30$	$L_n / 33$	$L_n / 33$
	520 MPa	$L_n / 28$	$L_n / 31$	$L_n / 31$
		ρ Slab without beams		
Eurocode 2 (2004)*	$\leq \rho_0$	L		
		$1.2 \left[11 + 1.5 \sqrt{f_c'} \frac{\rho_0}{\rho} + 3.2 \sqrt{f_c'} \left(\frac{\rho_0}{\rho} - 1 \right) \right]$		
	$> \rho_0$	L		
		$1.2 \left[11 + 1.5 \sqrt{f_c'} \frac{\rho_0}{\rho - \rho'} + \frac{1}{12} \sqrt{f_c'} \sqrt{\frac{\rho'}{\rho_0}} \right]$		
Scanlon and Lee (2006)		$L_n \left[\frac{480 \times 1.4 \times 1.35 (2W_s + W_L)}{16.7E_c} \right]^{1/3}$		

L = span; L_n = clear span, f_y = yield strength of reinforcement; $\rho_0 = 10^{-3} \sqrt{f_c'}$; ρ = tension reinforcement ratio; ρ' = compression reinforcement ratio; f_c' = concrete strength; W_s = sustained load; W_L = additional live load; and E_c = elastic modulus of concrete

* $L_{eff}/8.5$ should be multiplied to the calculated minimum slab thickness for a span of exceeding 8.5 m.

under construction load and the time-dependent deflection resulting from creep and shrinkage need to be estimated as accurately as possible. Fig. 1 shows the procedure of structural analysis proposed by Hwang *et al.* (2016) to predict slab deflections. In the analysis, the combined effect of the construction load, effective stiffness of early-age slabs, slab cracking, and creep and shrinkage of concrete can be considered.

The slab stiffness is reduced by cracking at each construction step (with load and time intervals). Thus, to determine the effective slab stiffness at each construction step, iterative calculations were used so that the total slab deflection is converged to a certain value. The time-dependent deflection at each construction step was defined as a sum of the creep deflection, which is a product of the creep coefficient and immediate deflection, and the shrinkage deflection. Then, the total deflection was calculated by accumulating the incremental immediate and time-dependent deflections of all previous construction steps.

2.3 Construction load

In order to calculate the construction load of shored slabs, the existing model of Park *et al.* (2011) was implemented in the analysis. Fig. 2 shows the idealized shored slab model for the construction load distribution: the construction loading step of casting new concrete at the top floor (Fig. 2(a)); and the subsequent loading step of removing shores at the bottom floor (Fig. 2(b)). In the floor slabs connected by shores, the floor construction load LS_i is distributed to each slab with a new construction load $Load_c$

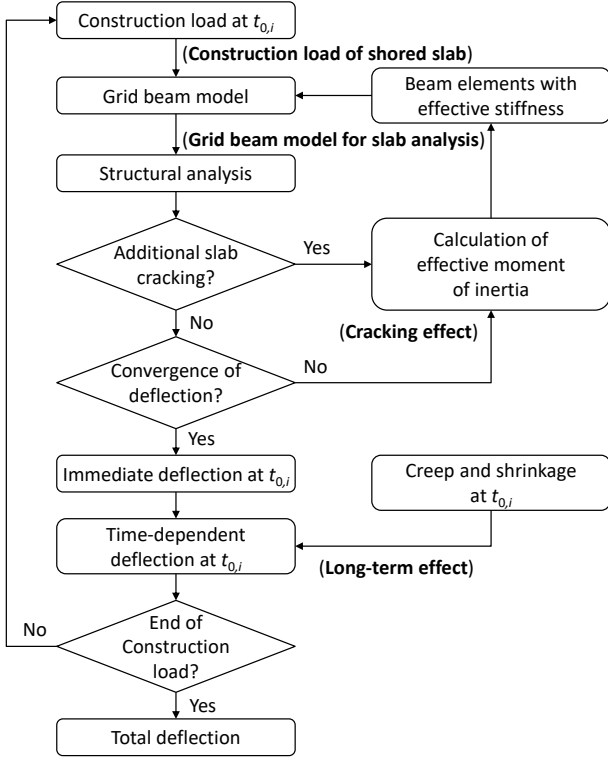


Fig. 1 Procedure of structural analysis

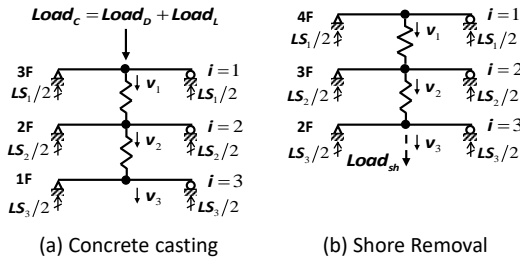


Fig. 2 Idealized shored slab model for construction load distribution

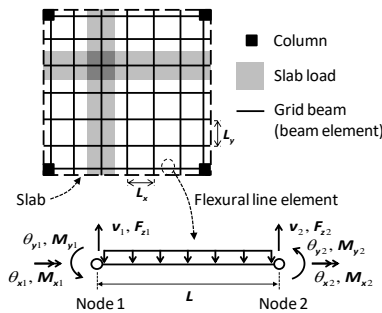


Fig. 3 Grid beam model for slab analysis

according to the relative stiffness of the slabs and shores (Eq. (1)).

$$\begin{pmatrix} LS_1 \\ LS_2 \\ \vdots \\ LS_{n_s} \end{pmatrix} = [K_{fst}] \begin{pmatrix} v_1 \\ v_2 \\ \vdots \\ v_{n_s} \end{pmatrix} = [K_{fst}][K_{ff}]^{-1} \begin{pmatrix} Load_C \\ 0 \\ \vdots \\ 0 \end{pmatrix} \quad (1)$$

where n_s = number of slabs resisting the superimposed load; $[K_{fst}]$ = effective stiffness matrix of slabs; v_i = equivalent deflection of each slab; and $[K_{ff}]$ = overall stiffness matrix of the idealized discrete system (Park *et al.* 2011). The effective stiffness of shored slabs is determined from the material properties of concrete (based on the construction cycle of each story), reduced stiffness of slabs with cracking, material property and spacing of shores (Park *et al.* 2011).

$$\begin{pmatrix} LS_1 \\ LS_2 \\ \vdots \\ LS_{n_s} \end{pmatrix} = [K_{fst}] \begin{pmatrix} v_1 \\ v_2 \\ \vdots \\ v_{n_s} \end{pmatrix} = [K_{fst}][K_{ff}]^{-1} \begin{pmatrix} 0 \\ 0 \\ \vdots \\ Load_{sh} \end{pmatrix} \quad (2)$$

In the same manner, the floor construction load LS_i by removing the bottom shores is distributed to each slab with $Load_{sh}$ according to the relative stiffness of the slabs and shores (Eq. (2)).

The construction load of each slab was calculated by accumulating the incremental construction loads of all construction steps.

2.4 Grid beam model for slab analysis

For two-way slab analysis, the flexural grid beam model of Hwang *et al.* (2016) shown in Fig. 3 was used. In the model, a two-way slab is idealized with flexural beam (or line) elements in x- and y-directions. The tributary area for calculating the load acting on each beam element is shown shaded in Fig. 3, and the uniform area load is converted into a uniformly distributed line load.

It is noted that the grid beam model was used only for one floor slab, because the interaction of multi-story slabs and the effect of shores were already taken into account in the calculation of the construction load. The reduced effective stiffness of early-age slabs under construction load and the moment redistribution due to cracking were calculated by iterations.

The flexural stiffness of each beam element is determined using the material properties of concrete at time t_0 when a new construction load is applied. The stiffness matrix of the beam element is given as Eq. (3), where F_{z1} and F_{z2} = nodal shear forces at both ends; M_{x1} and M_{x2} = nodal torsional moments; M_{y1} and M_{y2} = nodal flexural moments; $E_c(t_0)$ = elastic modulus of concrete at age t_0 ; $I(t_0)$ = moment of inertia of the beam element at age t_0 ; L = length of the beam element; $J(t_0) = (1-0.63x/y)x^3y/3$ = torsional constant of the beam element at age t_0 (Corley *et al.* 1970); x = short dimension of the beam section; y = long dimension of the beam section; $\nu = 0.2$ = Poisson ratio of concrete; v_1 and v_2 = nodal vertical displacements; θ_{x1} and θ_{x2} = nodal torsional angles; and θ_{y1} and θ_{y2} = nodal rotational angles.

$$\begin{pmatrix} F_{z1} \\ M_{y1} \\ M_{x1} \\ F_{z2} \\ M_{y2} \\ M_{x2} \end{pmatrix} = \frac{E_c(t_0)I(t_0)}{L} \begin{bmatrix} 12/L^2 & 0 & 6/L & -12/L^2 & 0 & 6/L \\ 0 & \frac{0.5J(t_0)}{(1+\nu)I(t_0)} & 0 & 0 & \frac{-0.5J(t_0)}{(1+\nu)I(t_0)} & 0 \\ 6/L & 0 & 4 & -6/L & 0 & 2 \\ -12/L^2 & 0 & -6/L & 12/L^2 & 0 & -6/L \\ 0 & \frac{-0.5J(t_0)}{(1+\nu)I(t_0)} & 0 & 0 & \frac{0.5J(t_0)}{(1+\nu)I(t_0)} & 0 \\ 6/L & 0 & 2 & -6/L & 0 & 4 \end{bmatrix} \begin{pmatrix} v_1 \\ \theta_{x1} \\ \theta_{y1} \\ v_2 \\ \theta_{x2} \\ \theta_{y2} \end{pmatrix} \quad (3)$$

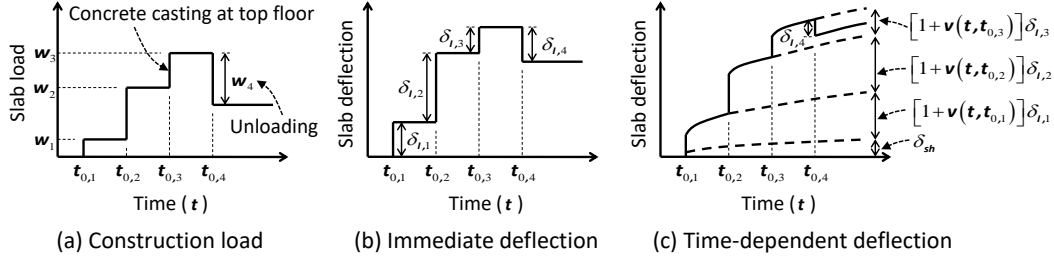


Fig. 4 Variations of slab load and deflection according to construction steps

2.5 Effective moment of inertia of slab

For slabs with reinforcement ratios of less than 1.0%, Eq. (4) of Bischoff and Scanlon (2007) can be used to define the effective moment of inertia I_e of the beam element (Lee *et al.* 2007, Park *et al.* 2012, Hwang *et al.* 2016).

$$I_e = \frac{I_{cr}}{1 - \left(\frac{M_{cr}}{M_a}\right)^2 \left(1 - \frac{I_{cr}}{I_g}\right)} \leq I_g \quad (4a)$$

$$M_{cr} = 0.63\sqrt{f'_c}I_g (2/h) \quad (4b)$$

where I_g = moment of inertia of the gross (uncracked) section; I_{cr} = moment of inertia of the cracked section; M_a = applied flexural moment; f'_c = concrete strength at the time when a new construction load is applied; and h = slab thickness.

Firky and Thomas (1988) define the moment of inertia I_{cr} of the cracked section as follows.

$$I_{cr} = \left[4k^3 + 12n\rho(1-k)^2\right] \left(\frac{d}{h}\right)^3 w_b I_g \quad (5a)$$

$$w_b = \left[6 \times 10^{-2} + 5\left(\frac{d'}{d}\right)\left(1 - \frac{2d'}{d}\right)^2\right] n\rho' \left(\frac{d'}{d}\right) + 1 \quad (5b)$$

where $k = \sqrt{2\rho n + (\rho n)^2} - \rho n$; ρ = tension reinforcement ratio ($= A_s/bd$); ρ' = compression reinforcement ratio ($= A_s'/bd$); n = modulus ratio of reinforcement to concrete; d = distance from the extreme compressive concrete fiber to the centroid of tension reinforcement; d' = distance from the extreme compressive concrete fiber to the centroid of compression reinforcement; and b = width of the beam element.

Fig. 4 shows the variations of the slab load and deflection according to construction steps. Since the effective moment of inertia depends on flexural moment and elastic modulus of concrete, it should be recalculated at every construction steps (i.e., considering construction load history and concrete age). The immediate deflection at each construction step is calculated as follows. 1) Linear analysis is performed for the uncracked section using Eq. (3) and concrete material properties at loading. 2) The effective moment of inertia of grid beam elements is evaluated using

the calculated moment distribution and Eqs. (4) and (5). Because the difference between the two end moments of each grid beam is generally not significant, the average value of the two end moments can be used in the evaluation of the effective moment of inertia. 3) Reanalysis is performed using the effective moment of inertia and Eq. (3). From this reanalysis, the slab moment is redistributed to grid beam elements. 4) Iterations of the analysis steps 2) and 3) are carried out until the slab deflection converges.

It is noted that flexural cracks reduce torsional resistance significantly. Thus, if cracking occurs ($I_e < I_g$), the torsional rigidity of grid beam elements can be neglected in the analysis for simple and conservative design. An increasing load history causes further damages (cracks), so the effective moment of inertia in the next construction step is generally less than that in the previous construction step. In the case of unloading (see w_4 in Fig. 4(a)), however, the slab deflection can be decreased by elastic recovery (neglecting creep recovery), which was confirmed from the previous analysis results and field measurements (Park *et al.* 2012, Hwang *et al.* 2016). Thus, at the unloading step, the gross moment of inertia I_g , instead of the effective moment of inertia I_e , is used for $I(t)$ in Eq. (3) for simplicity.

2.6 Creep and shrinkage of concrete

Slab deflections gradually increase with time due to creep (stress-dependent) and shrinkage (stress-independent) of concrete (Fig. 4(c)). In the present study, the prediction model of ACI 209R-92 (1992) was used to describe creep and shrinkage of concrete, because it gives good predictions for the time-dependent deflection of early-age slabs under construction loads (Park *et al.* 2012, Hwang *et al.* 2016). In the model, the creep coefficient $v(t, t_{0,i})$ and shrinkage strain $\varepsilon_{cs}(t)$ at time t are defined as follows.

$$v(t, t_{0,i}) = \frac{(t - t_{0,i})^{0.6}}{10 + (t - t_{0,i})^{0.6}} \times 2.35 \quad (6)$$

$$\times (\gamma_{c1} \cdot \gamma_{c2} \cdot \gamma_{c3} \cdot \gamma_{c4} \cdot \gamma_{c5} \cdot \gamma_{c6})$$

$$\varepsilon_{cs}(t) = \frac{(t - t_c)}{(35 + t - t_c)} \times (780 \times 10^{-6}) \quad (7)$$

$$\times (\gamma_{cs1} \cdot \gamma_{cs2} \cdot \gamma_{cs3} \cdot \gamma_{cs4} \cdot \gamma_{cs5} \cdot \gamma_{cs6} \cdot \gamma_{cs7})$$

where $t_{0,i}$ = concrete age at the i -th loading; γ_{c1} , γ_{c2} , γ_{c3} , γ_{c4} ,

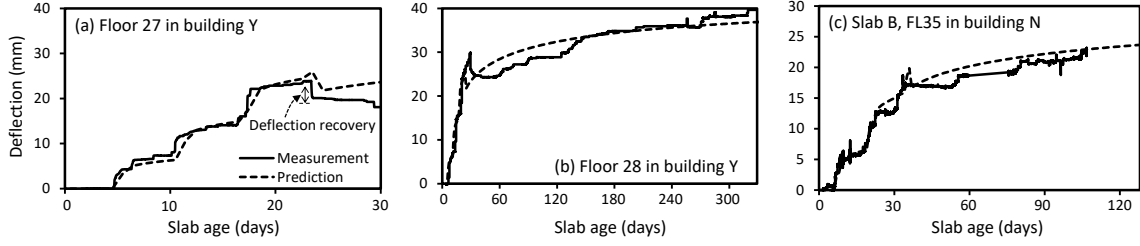


Fig. 5 Comparison of predictions and measured slab deflections

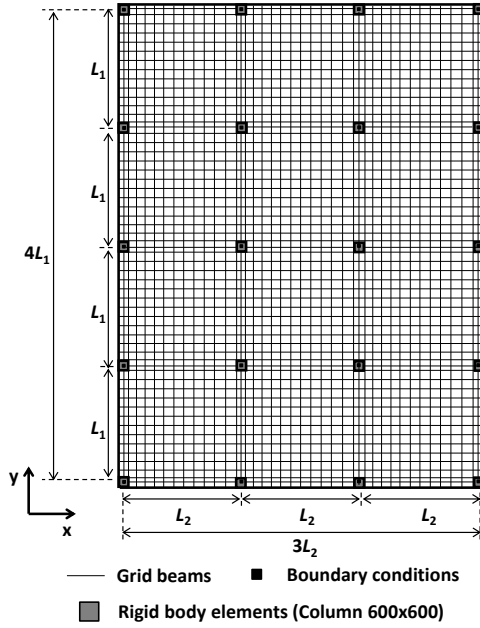


Fig. 6 Flat plate system for parametric study

γ_{c5} , and γ_{c6} = creep correction factors for loading age, ambient relative humidity, slab thickness, concrete slump, fine aggregate ratio, and air content; t_c = initial moist curing duration; and γ_{cs1} , γ_{cs2} , γ_{cs3} , γ_{cs4} , γ_{cs5} , γ_{cs6} , and γ_{cs7} = shrinkage correction factors for initial moist curing duration, ambient relative humidity, slab thickness, concrete slump, fine aggregate ratio, cement content, and air content, respectively.

The total deflection δ includes immediate, creep, and shrinkage deflections (Eq. (8)). The creep deflection is defined as a product of the immediate deflection and creep coefficient (ACI 209 1992). Since the immediate and creep deflections depend on stress, the total stress-dependent deflection can be calculated by adding all stress-dependent deflections of every construction loads (the first term in the right hand side of Eq. (8)).

$$\delta = \sum [1 + v(t, t_{0,i})] \delta_{I,i} + \delta_{sh} \quad (8)$$

where $\delta_{I,i}$ = immediate deflection at the i -th loading; and δ_{sh} = shrinkage deflection.

The shrinkage deflection δ_{sh} can be calculated by using the slab curvature $\phi_{sh}(t)$ corresponding to the immediate deflection. In the present study, the Branson's method (1963), which was introduced in ACI 209R-92 (1992), was used for the slab curvature (Eq. (9)). In the grid beam

model, the effective flexural stiffness for the shrinkage deflection was calculated from $EI_{eff} = M/\phi_{sh}(t)$ at the centroid of the cross-section, and then the shrinkage deflection was calculated using the effective flexural stiffness and Eq. (3).

$$\phi_{sh}(t) = \begin{cases} 0.7 \frac{\varepsilon_{cs}(t)}{h} \sqrt[3]{100(\rho - \rho')} \sqrt{\frac{\rho - \rho'}{\rho}}, & \rho - \rho' \leq 0.03 \\ \varepsilon_{cs}(t)/h, & \rho - \rho' > 0.03 \end{cases} \quad (9)$$

2.7 Verification of grid beam model

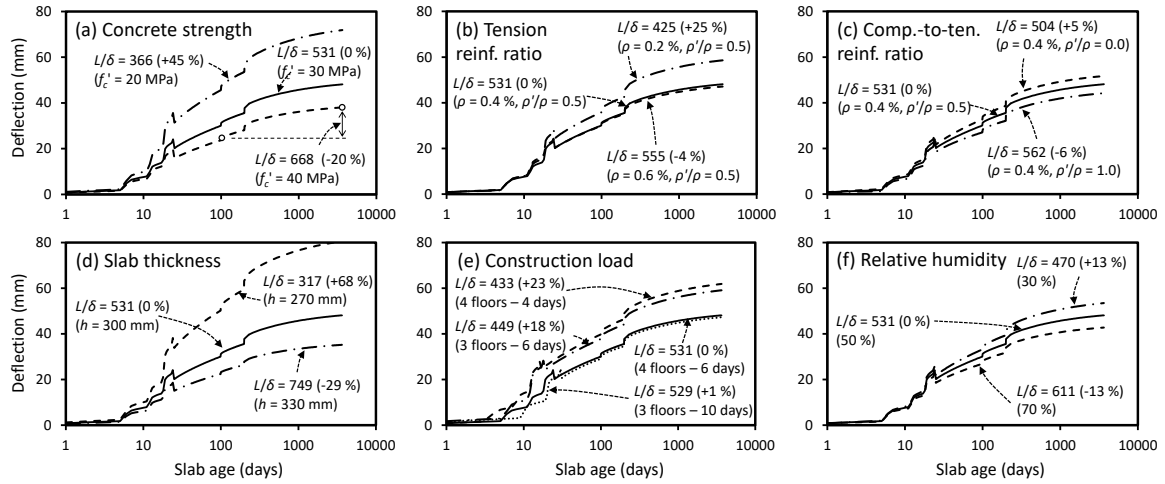
To verify the grid beam model, the predictions were compared with the measured slab deflections of actual long-span flat plate buildings Y and N under construction (Hwang *et al.* 2016). Detailed information of the actual buildings is available in the literature (Hwang *et al.* 2016). Fig. 5 shows the comparison. As shown in the figure, the predictions agreed well with the measured slab deflections.

3. Parametric analysis

To investigate the effects of design and construction parameters on slab deflections, a parametric study was performed for a flat plate system supported by columns only (Fig. 6). It is noted that in the parametric study, core walls were not considered. In general, a flat plate system is designed with a uniform slab thickness for constructability, and in that case, the slab thickness is controlled by the maximum deflection, which would happen far from core walls. Thus, for conservativeness, core walls were not considered.

The design parameters included the compressive strength of concrete ($f'_c = 20, 30, \text{ and } 40 \text{ MPa}$), tension reinforcement ratio ($\rho = 0.2, 0.4, \text{ and } 0.6\%$), compression-to-tension reinforcement ratio ($\rho'/\rho = 0, 0.5, \text{ and } 1.0$), and slab thickness ($h = 270, 300, \text{ and } 330 \text{ mm}$). The construction parameters included the construction load (shored floor – construction cycle = 3 floors – 6 days, 3 floors – 10 days, 4 floors – 4 days, and 4 floors – 6 days), and average ambient relative humidity ($RH = 30, 50, \text{ and } 70\%$).

Each floor measured 3.6 m in height and 9 m in span ($L_1 = L_2$). The elastic modulus of concrete was calculated by $E_c = 4700\sqrt{f'_c}$ (ACI 318 2014), and the elastic modulus of reinforcement was assumed to be 200 GPa. Spacing, cross-sectional area (per each), and elastic modulus of shores



* Default parameters : $f'_c = 30$ MPa; $\rho = 0.4\%$; $\rho'/\rho = 0.5$; $h = 300$ mm; shored floor – construction cycle = 4 floors – 6 days; relative humidity = 50 %

Fig. 7 Parametric study results for slab deflection

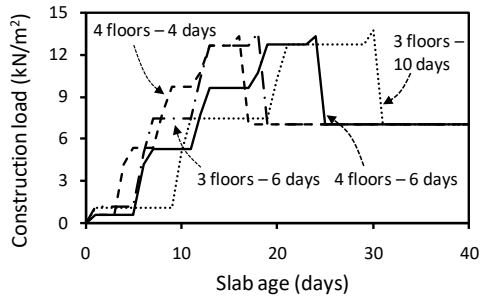


Fig. 8 Parametric study results for construction load

were 1300 mm, 500 mm², and 200 GPa. Following the construction practice in Korea, shores at the bottom floor were assumed to be removed 1 day after concrete casting at the top floor, and a finishing material load of 1.0 kN/m² and a live load of 2.0 kN/m² (for office use) were applied to each floor at 100 and 200 days after concrete casting, respectively (AIK 2016). The average temperature was assumed to be 20.0°C, and the analysis was performed for 10 years (3650 days). The default parameters are given in the bottom of Fig. 7.

Fig. 7 shows the parametric study results: slab deflections at corner spans (maximum). Generally, large deflections occurred at early ages (approximately during the first 24 days) due to construction loads, and the deflections were continuously increased after construction due to service loads and creep and shrinkage of concrete. For the total deflection occurring after attachment of nonstructural elements, ACI 318 (2014) requires that the span-to-deflection ratio L/δ be greater than 480 for serviceability. To check serviceability, L/δ resulting from the parametric study is provided in the figure, using the difference in deflection between 100 days (finishing) and 3650 days (10 years).

The concrete strength had a significant effect on the total deflection. As the concrete strength f'_c increased, the total deflection δ was decreased (Fig. 7(a)) due to the greater cracking resistance and effective stiffness of higher strength concrete: $L/\delta = 366$ for $f'_c = 20$ MPa, 531 for 30 MPa, or 668 for 40 MPa (compared with the deflection for

30 MPa, the deflection for 20 MPa was 45% larger, but the deflection for 40 MPa was 20% smaller). Only in the case of using 30 and 40 MPa, the total deflections satisfied the ACI requirement ($L/\delta \geq 480$). Under the same compression-to-tension reinforcement ratio ($\rho'/\rho = 0.5$), the total deflection was decreased as the tension (bottom) reinforcement ratio ρ increased. However, the effect of higher tension reinforcement ratios was limited, because the effective stiffness of slabs is not linearly increased with the increase of the reinforcement ratio: $L/\delta = 425$ for $\rho = 0.2\%$, 531 for 0.4%, or 555 for 0.6% (Fig. 7(b)). Under the same tension reinforcement ratio ($\rho = 0.4\%$), the total deflection was decreased, as the compression-to-tension reinforcement ratio ρ'/ρ increased: $L/\delta = 504$ for $\rho'/\rho = 0$, 531 for 0.5, or 562 for 1.0 (Fig. 7(c)). Compared with the effect of the tension reinforcement ratio (Fig. 7(b)), the effect of the compression (top) reinforcement ratio was less significant. This result was also reported in the previous test result for early-age slabs (Park *et al.* 2012). The slab thickness h had the most critical effect on the total deflection, because the effective stiffness of slabs is strongly affected by the slab thickness: $L/\delta = 317$ for $h = 270$ mm, 531 for 300 mm, or 749 for 330 mm (Fig. 7(d)).

Under the same design conditions ($f'_c = 30$ MPa, $\rho = 0.4\%$, $\rho'/\rho = 0.5$, and $h = 300$ mm), the total deflection varied with the construction conditions. The total deflection was affected by the construction load (shored floors-construction cycle). As the more floors were connected by shores (the smaller construction load on a floor) and/or the slower construction cycle was used (the higher strength and elastic modulus of concrete), the total deflection was decreased: $L/\delta = 449$ for 3 floors – 6 days, 529 for 3 floors – 10 days, 433 for 4 floors – 4 days, or 531 for 4 floors – 6 days (Fig. 7(e)). Fig. 8 shows the construction load histories of this case. Since the ambient relative humidity has an effect on creep and shrinkage, the total deflection was decreased, as the ambient relative humidity increased: $L/\delta = 470$ for $RH = 30\%$, 531 for 50%, or 611 for 70% (Fig. 7(f)).

These parametric study results confirm that the use of higher strength concrete, greater reinforcement ratio

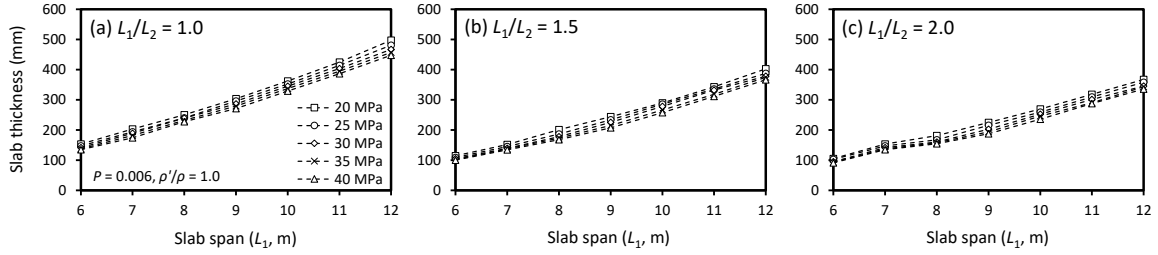


Fig. 9 Variation of minimum slab thickness with concrete strength

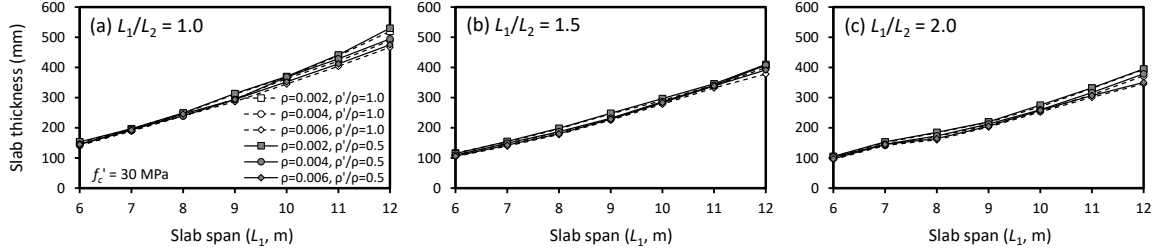


Fig. 10 Variation of minimum slab thickness with reinforcement ratio

(especially tension reinforcement), and thicker slab in design is desirable to decrease slab deflections. Further, construction conditions need to be considered in the calculation of slab deflections.

4. Minimum permissible thickness of slab

4.1 Derivation of minimum slab thickness

Since the requirement of ACI 318 (2014) for the minimum slab thickness is independent on loading and concrete modulus of elasticity and it could be unconservative in some cases (Lee and Scanlon 2010), the requirement needs to be improved. For design purpose, a new minimum permissible thickness of flat plate slabs is proposed satisfying the requirement of ACI 318 for the total deflection occurring after attachment of nonstructural elements (i.e., $L/\delta \geq 480$).

In order to cover general ranges of design conditions for flat plate slabs, the followings were considered: slab span = 6 to 12 m, long-to-short span ratio = 1.0 to 2.0, concrete strength = 20 to 40 MPa, tension reinforcement ratio = 0.2 to 0.6%, and compression-to-tension reinforcement ratio = 0.5 to 1.0. For construction conditions, which are difficult to be controlled at the design phase, the followings were assumed: 4 floors shored, 6-day construction cycle, shore removal after 1 day, average ambient relative humidity of 50%, finishing material load of 1.0 kN/m² at 100 days after concrete casting, and live load of 2.0 kN/m² at 200 days after concrete casting. By increasing the slab thickness for the various design conditions, the minimum slab thickness can be determined through numerical analysis.

Figs. 9 and 10 show the variations of the minimum slab thickness within the design conditions. As expected, as the span was the longer, the thicker slab was required. Further, the thicker slab was required for the smaller long-to-short span ratio (L_1/L_2) due to the two-way slab behavior, and the

effects of the concrete strength and reinforcement ratio were more pronounced in long spans. Thus, in the derivation of the minimum slab thickness, the effects of the slab span, span ratio, concrete strength, and reinforcement ratio need to be considered.

By definition, the total deflection δ after attachment of nonstructural elements can be divided into the stress-dependent (immediate plus creep) deflection δ_d due to dead load, stress-dependent deflection δ_l due to live load including finishing materials, and stress-independent (shrinkage) deflection δ_{sh} , and it should not be greater than the permissible limit δ_{lim} (Eq. (10)).

$$\delta = \delta_d + \delta_l + \delta_{sh} \leq \delta_{lim} \quad (10)$$

The stress-dependent deflection δ_d due to dead load can be defined as follows

$$\begin{aligned} \delta_d &= v_d K_d \frac{w_d L_n^4}{E_c I_e} \\ &= v_d K_d \left[\frac{\rho_c b (h - h_c) L_n^4}{E_c b (h - h_c)^3 / 12} + \frac{\rho_c b h_c L_n^4}{E_c b (h - h_c)^3 / 12} \right] \end{aligned} \quad (11)$$

where v_d = creep coefficient for dead load; K_d = coefficient for boundary conditions; w_d = slab weight; ρ_c = concrete density; b = effective slab width; and h_c = cracked thickness. In the right hand side bracket of Eq. (11), the first and second terms indicate the portions of the uncracked and cracked sections, respectively.

Substituting Eq. (11) into Eq. (10) gives Eq. (12a).

$$\begin{aligned} \delta_{lim} &\geq \\ v_d K_d &\left[\frac{\rho_c b (h - h_c) L_n^4}{E_c b (h - h_c)^3 / 12} + \frac{\rho_c b h_c L_n^4}{E_c b (h - h_c)^3 / 12} \right] + \delta_l + \delta_{sh} \end{aligned} \quad (12a)$$

The numerical analysis results for the general design conditions showed that the contributions of the deflections due to dead load, live load, and shrinkage to the total

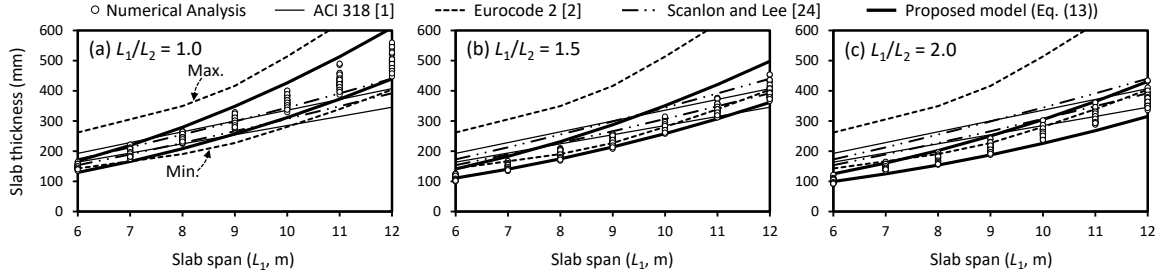


Fig. 11 Comparison of existing design methods for minimum slab thickness

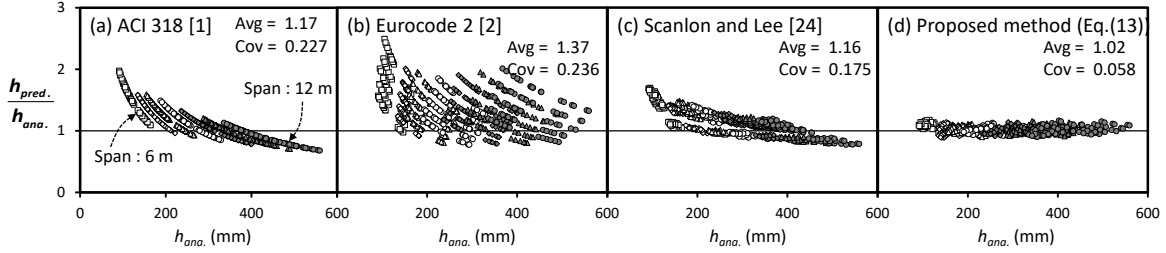


Fig. 12 Comparison of minimum slab thickness by existing design methods and numerical analysis

deflection are in the range of 53-58, 37-42, and 4-9%, respectively, and the portion of the uncracked section (the first term in the bracket of Eq. (12a)) counts for most of the deflection due to dead load. Thus, Eq. (12a) can be rewritten as follows.

$$\delta_{\text{lim}} - \left[\frac{v_d K_d \rho_c b h_c L_n^4}{E_c b (h - h_c)^3 / 12} + \delta_l + \delta_{sh} \right] \geq \left(\frac{v_d K_d \rho_c b}{E_c b / 12} \right) \frac{L_n^4}{(h - h_c)^2} \quad (12b)$$

By replacing the left hand side of Eq. (12b) with δ_c , Eq. (12b) can be expressed as a function of the clear span (L_n) and thickness ($h - h_c$) of the uncracked section (see Eq. (12c)).

$$\delta_c \left(\frac{E_c b / 12}{v_d K_d \rho_c b} \right) \geq \frac{L_n^4}{(h - h_c)^2} \quad (12c)$$

Finally, the proposed minimum slab thickness can be simplified as Eq. (13). In the equation, the empirical values C and h_c were obtained by regression analysis of the numerical analysis results (Figs. 9 and 10), and those two values implicitly reflect the effects of the construction load, reduced flexural stiffness and moment distribution of early-age slabs, and creep and shrinkage of concrete in the design equation.

$$h \geq \frac{L_n^2}{C} + h_c = \frac{(L_{n1}/100)^2}{0.4 f_c' + 16} \sqrt{\frac{L_{n2}}{L_{n1}}} \left(\frac{0.02}{\rho} + 0.95 \right) + 40 \quad (13)$$

(in mm and MPa)

where L_{n1} and L_{n2} = long and short clear spans ($L_{n1} \geq L_{n2}$). It is noted that Eq. (13) was derived assuming a conventional loading case for an office building (i.e., finishing material load of 1.0 kN/m² at 100 days after concrete casting, and

live load of 2.0 kN/m² at 200 days after concrete casting). For an exceptional case (e.g., extremely high load is imposed), the validity of the slab thickness should be verified by evaluation of slab deflections.

4.2 Comparison of existing design methods for minimum slab thickness

For comparison, the minimum slab thickness resulting from numerical analysis for the design conditions was compared with the predictions by existing design methods (ACI 318 2014, Eurocode 2 2004, Scanlon and Lee 2006 (Table 1)), and the proposed method (Eq. (13)).

Fig. 11 compares only the maximum and minimum values of the minimum slab thickness for each design method to show the range of variance. The ACI 318 model (2014) (for exterior panel without edge beams) gave a good prediction only for the case that the span is shorter than 8 m and the span ratio is $L_1/L_2 = 1.0$: it underestimated the minimum slab thickness for the longer spans (serviceability problems are possible to occur), while overestimated the minimum slab thickness for the greater span ratios (too conservative). As stated before, this is because that the ACI 318 model does not consider the effects of loading and elastic modulus of concrete. The Eurocode 2 model (2004) showed a wide range of variance by neglecting the construction load effect. Particularly, for the case of using lower strength concrete, the Eurocode 2 model significantly overestimated the minimum slab thickness. The Scanlon and Lee's model (2006) showed a narrow range of variance. However, it underestimated the minimum slab thickness for the case that the span is longer than 9 m and the span ratio is $L_1/L_2 = 1.0$, while overestimated the minimum slab thickness for the greater span ratios. On the other hand, the proposed model gave a good prediction for any cases, because it explicitly considers the slab span, span ratio, concrete strength, and reinforcement ratio.

Fig. 12 shows the relationship between numerical analysis results and predictions by existing design methods, and it reconfirms the exactness of the proposed method: the average ratio (Avg) of predictions to numerical analysis results and its coefficient of variation (Cov) were 1.17 and 0.227 for the ACI 318 model (2014), 1.37 and 0.236 for the Eurocode 2 model (2004), 1.16 and 0.175 for the Scanlon and Lee's model (2006), and 1.02 and 0.058 for the proposed method.

It is noted that the proposed method for the minimum slab thickness is valid only within the design and construction conditions described in the previous section. Other than these conditions, the proposed minimum slab thickness could not be satisfactory: for example, heavy and unexpected loads are applied after construction, or ambient conditions are more harsh (cold and dry regions).

5. Conclusions

To investigate immediate and time-dependent deflections of flat plate slabs, numerical analysis was performed considering the effects of the construction load of shored slabs, reduced flexural stiffness and moment distribution of early-age slabs, and creep and shrinkage of concrete. The construction load distribution of shored slabs was calculated by the idealized shored slab model, and the effective stiffness and moment distribution of slabs were calculated by the grid beam model. Then, the variations of the slab load and deflection according to construction steps (with load and time intervals) were calculated by iterations. The predictions by the numerical analysis method agreed well with the measured deflections. By using the numerical analysis method, a parametric study was performed for various design and construction conditions of practical ranges, and the parametric study results showed that the use of higher strength concrete, greater reinforcement ratio (especially tension reinforcement), and thicker slab in design is desirable to decrease slab deflections, and construction conditions also need to be considered in the calculation of slab deflections. Based on the numerical investigations, a new minimum permissible thickness of flat plate slabs was proposed satisfying the serviceability requirement of ACI 318 for the maximum total deflection occurring after attachment of nonstructural elements. The proposed minimum slab thickness and existing design methods were compared with numerical analysis results. The proposed equation gave a good prediction for any cases, while the existing design methods showed wide ranges of variance.

Acknowledgments

This research was financially supported by National Key Research Program of China (2016YFC0701400), National Natural Science Foundation of China (Grant No. 51650110500), and the Research Program funded by the SeoulTech (Seoul National University of Science and Technology). The authors are grateful to the authorities for their support.

References

- ACI Committee 209 (1992), *Prediction of Creep, Shrinkage, and Temperature Effects in Concrete Structures (ACI 209R-92)*, American Concrete Institute, Farmington Hills, Michigan, U.S.A.
- ACI Committee 318 (2014), *Building Code Requirements for Structural Concrete and Commentary (ACI 318-14)*, American Concrete Institute, Farmington Hills, Michigan, U.S.A.
- ACI Committee 347 (2005), *Guide for Shoring/Reshoring of Concrete Multistory Buildings (ACI 347.2R-05)*, American Concrete Institute, Farmington Hills, Michigan, U.S.A.
- AIK (2016), *Korean Building Code*, Architectural Institute of Korea, Kimundang, Seoul, Republic of Korea.
- Bischoff, P.H. and Scanlon, A. (2007), "Effective moment of inertia for calculating deflections of concrete members containing steel reinforcement and fiber-reinforced polymer reinforcement", *ACI Struct. J.*, **104**(1), 68-75.
- Branson, D.E. (1963), *Instantaneous and Time-Dependent Deflections of Simple and Continuous Reinforced Concrete Beams*, Alabama Highway Research Department, Bureau of Public Roads, Report No.7, Part I, 1-78.
- Carino, N.J. and Lew, H.S. (1983), "Temperature effects on strength-maturity relations of mortar", *ACI J. Proc.*, **80**(3), 177-182.
- CEB-FIP (1993), *CEB-FIP Model Code 1990: Design Code*, Euro-International Committee for Concrete, Thomas Telford, London, U.K.
- CEN (2004), *Eurocode 2: Design of Concrete Structures-Part 1-1: General Rules and Rules for Buildings*, European Committee for Standardization, Brussels, Belgium.
- Corley, W.G. and Jirsa, J.O. (1970), "Equivalent frame analysis for slab design", *ACI J.*, **67**(11), 875-884.
- El-Shahhat, A.M. and Chen, W.F. (1992), "Improved analysis of shore-slab interaction", *ACI Struct. J.*, **89**(5), 528-537.
- Firky, A.M. and Thomas, C. (1988), "Development of a model for the effective moment of inertia of one-way reinforcement concrete elements", *ACI Struct. J.*, **95**(4), 444-455.
- Gardner, N.J. and Fu, H.C. (1987), "Effects of high construction loads on the long-term deflections of flat slabs", *ACI Struct. J.*, **84**(3), 349-360.
- Gilbert, R.I. (1999), "Deflection calculation for reinforced concrete structures-why we sometimes get it wrong", *ACI Struct. J.*, **96**(6), 1027-1033.
- Grundy, P. and Kabaila, A. (1963), "Construction loads on slabs with shored formwork in multistory buildings", *ACI J. Proc.*, **60**(12), 1729-1738.
- Hossain, T.R. and Vollum, R.L. (2002), "Prediction of slab deflections and validation against cardington data", *Proceedings of the ICE-Structures and Buildings*, **152**(3), 235-248.
- Hossain, T.R., Vollum, R.L. and Ahmed, S.U. (2011), "Deflection estimation of reinforced concrete flat plates using ACI method", *ACI Struct. J.*, **108**(4), 405-413.
- Hwang, H.J., Park, H.G., Hong, G.H., Kim, J.Y. and Kim, Y.N. (2016), "Time-dependent deflection of slab affected by construction load", *ACI Struct. J.*, **113**(3), 557-566.
- Kang, S., Choi, K. and Park, H. (2003), "Minimum thickness requirements of flat plate affected by construction load", *J. Kor. Concrete Inst.*, **15**(5), 650-661.
- Kim, J. (2009), "Applications of practical analysis scheme for evaluating effects of over-loads during construction on deflections of flat plate system", *J. Comput. Struct. Eng. Inst. Kor.*, **22**(1), 25-34.
- Kim, J.Y. and Kang, S.M. (2017), "Simulations of short-and long-term deflections of flat plates considering effects of construction sequences", *Struct. Eng. Mech.*, **62**(4), 477-485.
- Lee, J.I., Scanlon, A. and Scanlon, M.A. (2007), "Effect of early

- age loading on time-dependent deflection and shrinkage restraint cracking of slabs with low reinforcement ratios”, *Struct. Implicat. Shrinkag. Creep Concrete, Am. Concrete Inst.*, SP-246-9, 149-166.
- Lee, Y.H. and Scanlon, A. (2010), “Comparison of one- and two-way slab minimum thickness provisions in building codes and standards”, *ACI Struct. J.*, **107**(2), 157-163.
- Liu, X., Chen, W.F. and Bowman, M.D. (1985), “Construction load analysis for concrete structures”, *J. Struct. Eng.*, **111**(5), 1019-1036.
- Mehta, P.K. and Monteiro, P.J.M. (2006), *Concrete Microstructure, Properties, and Materials*, 3rd Edition, McGraw-Hill, New York, U.S.A.
- Mosallam, K.H. and Chen, W.F. (1991), “Determining shoring loads for reinforced concrete construction”, *ACI Struct. J.*, **88**(3), 340-350.
- Park, H., Hwang, H., Hong, G., Kim, Y. and Kim, J. (2011), “Slab construction load affected by shore stiffness and concrete cracking”, *ACI Struct. J.*, **108**(6), 679-688.
- Park, H., Hwang, H., Hong, G., Kim, Y. and Kim, J. (2012), “Immediate and long-term deflections of reinforced concrete slab affected by early-age loading and low temperature”, *ACI Struct. J.*, **109**(3), 413-422.
- Scanlon, A. and Lee, Y.H. (2006), “Unified span-to-depth ratio equation for non-prestressed concrete beams and slabs”, *ACI Struct. J.*, **103**(1), 142-148.
- Vollum, R.L., Moss, R.M. and Hossain, T.R. (2002), “Slab deflections in the cardington in-situ concrete frame building”, *Mag. Concrete Res.*, **54**(1), 23-34.